AAPS PharmSciTech, Vol. 19, No. 4, May 2018 (© 2018)
DOI: 10.1208/s12249-018-1004-5

Research Article

Zein Microneedles for Localized Delivery of Chemotherapeutic Agents to Treat Breast Cancer: Drug Loading, Release Behavior, and Skin Permeation Studies

Shubhmita Bhatnagar,[1] Pooja Kumari,[1] Srijanaki Paravastu Pattarabhiran,[1] and Venkata Vamsi Krishna Venuganti[1,2]

Received 29 January 2018; accepted 19 March 2018; published online 3 April 2018

Abstract. Localized delivery of chemotherapeutic agents to treat breast cancer could limit their adverse drug reactions. The aim of this study was to investigate the influence of physicochemical properties of chemotherapeutic agents in their loading, release behavior, and skin permeation using microneedles. Zein microneedles were fabricated using the micromolding technique containing 36 microneedles in a 1-cm^2 area. These microneedles were loaded with two anti-breast cancer drugs, tamoxifen and gemcitabine, having different water solubilities. Entrapment or surface coating of chemotherapeutic agents in zein microneedles was optimized to achieve greater loading efficiency. The greatest loading achieved was 607 ± 21 and 1459 ± 74 μg for tamoxifen and gemcitabine using the entrapment approach, respectively. Skin permeation studies in excised porcine skin showed that the coating on microneedles approach results in greater skin deposition for tamoxifen; while the poke-and-patch approach would provide greater skin permeation for gemcitabine. Taken together, it can be concluded that different loading strategies and skin penetration approaches have to be studied for delivery of small molecules using polymeric microneedles.

KEY WORDS: tamoxifen; gemcitabine; zein microneedles; drug release; skin permeation.

INTRODUCTION

Microneedle-based devices are poised to disrupt the way therapeutics are administered in a localized region (1,2). Microneedles have shown potential in their utility as devices for disease diagnosis, drug and vaccine delivery, and cosmetic application (3). Despite the research efforts on microneedles diversified into finding better production technologies, optimized needle dimensions, and modes of insertion into tissues, the material of construction has emerged as the most important parameter that affects drug delivery (4–6). Micromachining tools have been used to fabricate microneedles made of stainless steel, silicon, and ceramic materials (7,8). However, their application in drug delivery is limited by poor drug loading efficiency. The metal-based microneedles would generally be applicable in the poke-and-patch approach, where blank microneedles are inserted into the skin, and then the drug formulations are applied to allow drug permeation (9). The amount of drug that can be coated onto the metal-based needle materials is severely limited (10). An alternative to the use of metal-based materials is to prepare hollow microneedles. The liquid drug formulation can be transported into the skin through the hollow needles (4). However, this is limited by the fluid volume that can be administered and the skin resistance against permeation of fluids.

In the second generation of microneedle development, the micromolding technique allowed utilization of varied polymeric materials to construct microneedles (6,11,12). This has significantly expanded the scope of application of microneedles to diversified areas. Some of the most widely used polymeric materials to construct microneedles have been polyvinyl alcohol, polyvinyl pyrrolidone, sodium carboxy methyl cellulose, chitosan, alginate, poly(β-ester), acrylate polymers, and polylactide, among others (13). These polymeric microneedles could be tailored to be stable or dissolvable and optimize the drug loading and release behavior (11,14,15).

In general, the polymer and casting medium characteristics including molecular weight, water solubility, concentration, viscosity, and entrapped air would influence the mechanical strength, skin insertional force, and stability of microneedles (16,17). Furthermore, these material attributes

Pooja Kumari and Srijanaki Paravastu Pattarabhiran contributed equally to this work.

Electronic supplementary material The online version of this article (https://doi.org/10.1208/s12249-018-1004-5) contains supplementary material, which is available to authorized users.

[1] Department of Pharmacy, Birla Institute of Technology and Science (BITS) Pilani, Hyderabad Campus, Hyderabad, Telangana 500078, India.

[2] To whom correspondence should be addressed. (e–mail: vamsi@hyderabad.bits-pilani.ac.in)

would also influence the amount of drug that can be loaded within microneedles or coated on the microneedle surface (18,19).

To that end, the objective of this study was to understand the influence of water solubility of compounds in their entrapment, release behavior, and skin permeation in zein microneedles. Zein is a prolamine protein derived from corn. It is generally regarded as safe (GRAS) material by US-FDA that is used in the manufacture of biodegradable plastics, fibers, coatings, adhesives, and inks (20). Earlier, we have reported development of zein microneedles to deliver antigen for transcutaneous immunization (11). Zein microneedles have not been studied for delivery of small molecules. Here, we report the loading of two widely used anti-breast cancer agents, tamoxifen and gemcitabine, in zein microneedles. These two drugs possess different water solubilities. The physico-chemical properties of tamoxifen included molecular weight, 371.5 Da; melting point, 95°C; water solubility, 0.04 μg/ml; log P, 4.44; pK_a, ~8.8; and clinical dose requirement, 20–40 mg/day (21–25). On the other hand, the physico-chemical properties of gemcitabine included molecular weight, 299.6 Da; melting point, 277°C; water solubility, ~38 mg/ml; log *P*, (−)1.4; pK_a, 3.6; and a clinical dose requirement of 800–1250 mg/m^2 (26–30). The influence of these properties in their skin permeation after loading in microneedles was studied.

MATERIALS AND METHODS

Materials

Tamoxifen was purchased from Sigma-Aldrich (Bangalore, India). Gemcitabine hydrochloride was a gift sample from Fresenius Kabi India Pvt. Ltd., Gurgaon, India. Zein, polyethylene glycol 400 (PEG 400), glycerol, rhodamine B base, and all other chemicals were purchased from Sigma-Aldrich Chemical Company (Bengaluru, India). PVP-K30 was obtained from Himedia Laboratories, Mumbai. Isopropyl alcohol, HPLC-grade acetonitrile, methanol, and ammonium acetate were procured from ThermoFisher Scientific. Milli-Q (Millipore, USA) water was used for all the experiments.

Preparation of Drug-Entrapped Microneedles

Zein microneedles (ZMN) were fabricated using the micromolding technique as described in our earlier report (11). Briefly, a master mold with 6 × 6 array design was 3D printed with acrylobutyl nitrile styrene (ABS) polymer. This master mold was used to prepare needle-free polydimethyl siloxane (PDMS) molds. Zein protein (60% *w*/*w*) in 90% ethanol was used to prepare ZMN. Glycerol and PEG 400 at 10% *w*/*w* concentrations were used as plasticizers. The tamoxifen- and gemcitabine-entrapped ZMN were prepared by mixing the drugs at 1:100 *w*/*w* of zein and 25 mg, respectively, before casting the needles. Free or drug-entrapped zein matrix was poured onto the PDMS mold and allowed to settle in the pores under vacuum. Then, the molds were allowed to air-dry for 48 h after which they were gently peeled.

Preparation of Drug-Coated Microneedles

Blank ZMN were prepared as described in the previous section. These blank ZMN were dip coated with either tamoxifen or gemcitabine. ZMN were dipped into the drug solution in a controlled fashion by attaching the array to the arm of a texture analyzer setup (Stable Microsystems, UK). To optimize the coating, the dipping medium was prepared using different concentrations of PVP including 10, 20, 30, 40, and 50% *w*/*v* in 100% ethanol. Rhodamine (1 mg/ml) was used as a model dye to visualize the coating characteristics. ZMN were coated with rhodamine–PVP solution using the texture analyzer setup with a 30-s dip time. Tamoxifen was coated on ZMN using tamoxifen (5 mg/ml) dissolved in 30% *w*/*v* PVP. The needles were dipped in coating solution for 30 s and air-dried for 12 h. Similarly, gemcitabine was coated on ZMN by dipping in 42 mg/ml gemcitabine in phosphate buffer.

Characterization of Drug-Loaded ZMN

ZMN were examined for needle dimensions and uniformity using an optical microscope (IX53, Olympus, Japan). PVP–rhodamine-coated microneedles were imaged using a stereomicroscope (SZX2, Olympus, Japan) and fluorescence microscope (DMi8, Leica, Germany). A texture analyzer (TA XT, Stable Microsystems, UK) was used to measure the compression force required to fail ZMN. A cylindrical Delrin probe (10 mm, part code P/10) linked to a 50-kg load cell was set in the compression mode, while ZMN were placed on a heavy metal platform. The probe compressed the microneedle array with a speed of 0.5 mm/s up to a distance of 0.8 mm. Then the probe was held in place for 5-s. Compression force *vs.* distance plots were recorded for three sets of ZMN.

FTIR and a differential scanning calorimeter (DSC) were used to study the drug loading in ZMN. For FTIR (FT/IR-4200, Jasco Inc., USA) studies, spectra were obtained for neat tamoxifen, gemcitabine, zein, physical mixtures (zein + gemcitabine, zein + tamoxifen), blank, and drug-loaded ZMN. The samples were mixed with potassium bromide in a 1:1 weight ratio, and spectra were recorded between wavenumbers 4000 and 400 cm^{-1} at a resolution of 2 cm^{-1} in a dynamic reflectance sample holder. For drug-loaded ZMN, three needles from the array were carefully cut using a scalpel and mixed with potassium bromide to prepare the pellet. For the same preparations, DSC (DSC 60, Shimadzu, Japan) was used to investigate the thermal transitions. Samples (2 mg) were placed in aluminum pans and hermetically sealed. Thermograms were recorded between ambient temperature and 300°C with a constant heating rate of 10°C per minute. To record thermogram for microneedles, three needles were cut from the array and hermetically sealed in an aluminum pan.

HPLC Method for Tamoxifen and Gemcitabine

The reverse-phase HPLC (LC-20, Shimadzu, Japan) method was developed for quantification of tamoxifen and gemcitabine. For tamoxifen analysis, a combination of 0.5 mM ammonium acetate and methanol (15:85) was used as mobile phase. The chromatographic separation of

tamoxifen (50 μl injection volume) was achieved on an end-capped C18 analytical column (150 × 4.6 mm i.d., 5 μm, Phenomenex, USA), maintained at 40°C at a 1-ml/min flow rate. The absorbance was recorded at 274 nm wavelength using a UV–visible detector. Standard concentrations of tamoxifen were prepared at 0.5, 1, 2, 4, 6, and 8 μg/ml in methanol ($n = 6$). The regression equation was obtained by plotting the area under the curves against concentrations ($y = 89{,}254x + 9976.9$; $r^2 = 0.9993$). For gemcitabine analysis, the mobile phase included a combination of phosphate buffer pH 7.4 and methanol at a 90:10 ratio. The column temperature was maintained at 10°C. The injection volume was 40 μl, and the flow rate was maintained at 1 ml/min. Absorbance corresponding to gemcitabine was recorded at 275 nm wavelength. Standard concentrations of 5, 10, 15, 25, and 30 μg/ml ($n = 6$) were prepared in phosphate buffer to obtain the regression equation ($y = 41{,}697x + 387$; $r^2 = 0.9999$).

Drug Release Studies

The Franz diffusion cell setup (PermeGear Inc., USA) was used to perform the drug release studies. ZMN entrapped or coated with tamoxifen and gemcitabine were placed with needles facing down at the interface of donor and receptor chamber such that the needles were freely immersed in receptor medium. The receptor chamber contained phosphate-buffered saline (PBS, pH 7.4, 5 ml) that was mixed using a magnetic stir bar. Tamoxifen release studies also contained 20% methanol in the receptor chamber to improve solubility. At predetermined time points, a 300-μl sample was withdrawn from the receptor chamber and restored with fresh medium. Samples were analyzed using the HPLC method described above.

ZMN/release medium partitioning studies were performed to understand the partitioning of drugs into the zein matrix. Tamoxifen (1 μg/ml) and gemcitabine (0.3 mg/ml) drug solutions were prepared in PBS:methanol (80:20) and PBS, respectively. Blank ZMN were incubated in drug solution for 24 h at 37°C. Then, the concentration of drug in the aqueous phase was analyzed using HPLC. The ratio of drug concentration in ZMN to the release medium was calculated.

In Vitro Skin Penetration Studies

Excised porcine ear skin was used as a model to study ZMN insertion and drug permeation into and across skin. Porcine ears were purchased from a local abattoir. The ears were rinsed with water, and hair on the dorsal surface was trimmed using a hair trimmer. The dorsal ear skin was harvested using a scalpel blade, and any remaining subcutaneous fat was carefully removed. Excised skin was stored at − 80°C and used within 3 months for experimentation. During the experiment, the skin was thawed at room temperature and stabilized at 37°C for 3 h. Skin sample thickness was gauged using a digital micrometer (Baker Gauges India Pvt. Ltd., Mumbai, India). The skin sample was mounted in a Franz diffusion cell by sandwiching it between the donor and the receptor chamber with the epidermis facing the donor chamber. The transepidermal electrical resistance (TEER) of the skin was measured by applying 1 mA of direct current (I) across the skin with a DC power source. The dip in voltage (V) was gauged using a digital multimeter (17B, Fluke Corporation, WA, USA). Using Ohm's law ($V = IR$), the resistance (R) was calculated. Only skin samples with TEER > 3 kΩ were used in the study. Transepidermal water loss (TEWL) of skin samples was measured using a VapoMeter® (Delfin Technologies Ltd., Kuopio, Finland). TEWL was measured by placing the probe over the donor chamber of the diffusion cell.

Three different experimental approaches were performed to study the drug permeation through skin using ZMN. For the "poke-and-patch" approach, ZMN were inserted into skin and held for 5 min. ZMN were pressed onto the skin sample with slight thumb pressure. The pressure and duration were fixed based on our previous report with similar ZMN that was sufficient for skin insertion (11). This poked skin was charged with 200 μl of drug solution (0.5 mg/ml) in the donor chamber and treated for 48 h. In the other two approaches, ZMN entrapped or coated with drugs were inserted into skin and treated for 48 h. Samples (0.3 ml) were withdrawn from the receptor chamber at predetermined time points and analyzed using the HPLC method described above. After 48 h, the ZMN were withdrawn and skin samples were dabbed with Kimwipes to remove surface-adsorbed compound. The tape stripping technique was performed to remove the stratum corneum layer using Scotch book tape (845, 3M Corporation, USA). Fifteen strips were collected to remove the stratum corneum. TEER and TEWL were measured before and after tape stripping. Tamoxifen and gemcitabine from tape strips were extracted by incubation in methanol or phosphate buffer, respectively, for 12 h while shaking. Viable skin remained after stripping was cut into small pieces using a sharp blade and homogenized using a tissue homogenizer. Tamoxifen and gemcitabine were extracted by incubation in methanol or phosphate buffer, respectively, for 12 h. All the samples were subjected to HPLC analysis. It should be noted that the amount of drug charged in the donor chamber for the three approaches was different. The release percentages were calculated based on the total amount of drug loaded within entrapped or coated ZMN.

In a different experiment, tamoxifen–PVP-coated ZMN or gemcitabine-coated ZMN were inserted into the skin for 5 min. The skin samples were processed to determine the amount of tamoxifen retained within the stratum corneum and viable epidermis as described above.

Skin permeation parameters were calculated by plotting the cumulative amount of drug permeated per unit area of skin against time. Flux (J) was obtained from the slope of the linear part of the curve. The lag time (t_{lag}) was calculated from the reverse extrapolation of the steady-state portion of the curve to the time axis. The permeability coefficient (K_p) and diffusion coefficient (D) were computed using Eqs. (1) and (2):

$$Kp = \frac{J}{C_d} \tag{1}$$

$$D = \frac{h^2}{6 \times t_{lag}} \tag{2}$$

where C_d is the concentration of the drug in the donor compartment and h is the thickness of the skin.

Statistical Analysis

All the results were reported as average ± standard deviation ($n \geq 3$). The results were correlated by performing Student's t test or analysis of variance (GraphPad Prism, USA), where $p < 0.05$ was considered to be significant, unless specified.

RESULTS

Characterization of ZMN

Figure 1 shows the scheme for fabricating ZMN. Figure 1a, b shows a 3D-printed ABS mold and PDMS mold, respectively. Figure 1c shows a stereomicroscope image of the microneedle array. The microscopic image of a single needle is shown in Fig. 1d. The ZMN were smooth conical structures with an average length and width at the base of 965 ± 23 and 363 ± 15 μm, respectively. No observable stress marks could be seen on the needle surface. Drugs were loaded in ZMN by either entrapping into the matrix or coating onto the needles. Figure 1e depicts the procedure for preparing drug-entrapped and drug-coated microneedles. The dipping method was used to prepare the drug-coated microneedles (Fig. 1e).

The coating solution was optimized for PVP (10–50% *w/v* in ethanol) concentration to prepare tamoxifen-coated microneedles. Figure 2a, b shows representative fluorescence and brightfield microscopic images of PVP–rhodamine-coated ZMN, respectively. The shape of the microneedles was retained after coating with 10, 20, and 30% *w/v* PVP with uniform coating. Coating with higher PVP concentrations (40 and 50% *w/v*) led to excess deposition on the needle tips that resulted in blunt bulb structures (Fig. 2b). Figure 2c shows the compression force *versus* displacement plots for the drug-coated ZMN. The compression force increased with the increase in the PVP concentration in the coating solution. A compression force of 16.1 ± 1.5 N was recorded for blank ZMN. A PVP concentration of 30% *w/v* has shown the integrity of the needle shape and the spread deposition with suitable mechanical strength. Therefore, 30% *w/v* PVP was used as an optimized dipping medium for tamoxifen coating on ZMN. On the other hand, gemcitabine, being a water-soluble compound, was dip coated without using a hydrophilic polymer coating solution. Gemcitabine-coated or entrapped ZMN showed similar compression force as blank ZMN (Supplementary Fig. S1). All the force–displacement curves were smooth, indicating no abrupt buckling or breaking of microneedle tips (Supplementary Fig. S1).

Figure 3 shows representative DSC thermograms of neat zein, gemcitabine, tamoxifen, and their physical mixtures and after entrapment in ZMN. Tamoxifen and gemcitabine showed an endothermic peak at 95 and 277.5°C temperature, respectively, indicating their crystalline nature. No characteristic peak was observed for neat zein up to a temperature of 300°C. The physical mixtures of zein–tamoxifen and zein–gemcitabine and drug-entrapped ZMN did not show the endothermic transitions correlating to tamoxifen and gemcitabine. This could be because of the low entrapment of the drugs within ZMN. Figure 4 shows the representative FTIR spectra of the neat compounds and their physical mixtures. Zein showed its characteristic amide peaks between 1500 and 1700 cm^{-1} (1664 and 1550 cm^{-1} for amide I and amide II, respectively). The FTIR spectrum of gemcitabine showed characteristic peaks at 1680, 1721, and 3393 cm^{-1} corresponding to amine bands, ureido group, and NH_2 stretching vibration. The spectrum for neat tamoxifen exhibits characteristic peaks at 1610 cm^{-1} (C=C stretching) and 1512 cm^{-1} (C=C aromatic ring stretching). C–O aryl ethers stretching bands could be seen at 1246 and 1033 cm^{-1}. The spectra of physical mixtures and drug-entrapped ZMN showed peaks as similar wave numbers.

Drug Loading and Release Profile

The average amount of tamoxifen entrapped in each microneedle array was 607 ± 21 μg. Tamoxifen drug release studies were performed in phosphate buffer and phosphate buffer containing ethanol/ methanol mixture. Tamoxifen release from ZMN was negligible at 1.2% after 12 h (Fig. 5).

Tamoxifen was coated on the ZMN to improve the percentage drug release. Different coating media were used to optimize the loading of tamoxifen. Initially, dip coating was performed using tamoxifen dissolved in 1% ethyl cellulose in isopropyl alcohol. The average amount of 208 μg tamoxifen was coated in each microneedle array. However, only 1% tamoxifen was released over a period of 12 h. Then, different concentrations of PVP in ethanol were used to coat tamoxifen over ZMN. PVP (30% *w/v* in ethanol) solution containing 35 mg/ml tamoxifen was used as optimized coating solution. Needles were cut from the MN bases, and the drug coated onto needles and bases was estimated separately. The amount of tamoxifen coated onto the base and needles was 320.7 ± 52.7 and 158.1 ± 44.9 μg, respectively. The loading efficiency and entrapment efficiency (EE) was calculated using Eqs. 3 and 4, respectively.

$$\%\text{loading efficiency} = \frac{\text{amount of drug in ZMN array}}{\text{average weight of ZMN array}} \times 100 \quad (3)$$

$$\%\text{EE} = \frac{\text{amount of drug coated on 36 needles}}{\text{amount of drug in coating solution used for ZMN array}} \times 100 \quad (4)$$

For tamoxifen-entrapped ZMN, the loading and entrapment efficiency was found to be 0.170 ± 0.005 and 100%, respectively. The entrapment efficiency would be 100% as ZMN were prepared by the solvent casting method. Similarly, for tamoxifen-coated ZMN, the loading and entrapment efficiency was found to be 4.59 ± 1.30 and 4.55 ± 0.50%, respectively. Drug release studies showed that after the 15-min time point, 80% of the microneedle loaded tamoxifen was released into the receptor medium. Surprisingly, this cumulative amount released decreased with progression of time and showed 8.67 ± 1.14% in the receptor medium after 48 h. It was found that 89.46 ± 7.63% of loaded tamoxifen remained in the microneedle array after 48 h. Several repetitions of this release study showed a similar profile (Fig. 5). It can be concluded that tamoxifen partitioned back into the zein microneedle matrix after the initial burst release. This initial burst release is attributed to the water-soluble

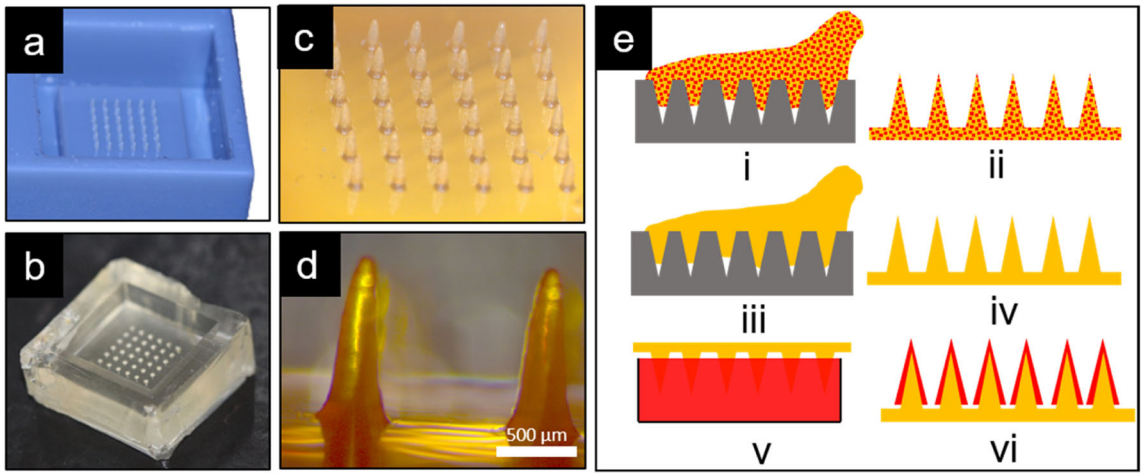

Fig. 1. Representative photographs of 3D-printed **a** ABS mold and **b** PDMS mold and **c** microneedle array. **d** Optical micrograph of a single microneedle (scale bar—0.5 mm). **e** Scheme of fabrication of drug-entrapped (i–ii) and drug-coated (iii–vi) microneedles. The drug-incorporated matrix is poured onto PDMS molds (i) to form drug-entrapped microneedles (ii) or blank microneedles (iv) are dipped into coating solution (v) to give drug-coated microneedles (vi)

PVP used in the coating solution. The tamoxifen partitioning studies in the ZMN-aqueous release medium showed that tamoxifen was completely partitioned into ZMN, while no drug was detectable in the release medium after 24 h incubation.

Another anti-cancer agent, gemcitabine, with greater water solubility compared with tamoxifen was entrapped or coated onto ZMN. The amount of gemcitabine entrapped into microneedles was 1458.55 ± 73.57 µg. Drug loading and entrapment efficiency was found to be 0.41 ± 0.02 and 100%, respectively. Gemcitabine was coated onto ZMN using gemcitabine dissolved in phosphate buffer. It was found that 83.07 ± 3.24 µg of gemcitabine was coated onto the microneedles (only 3.86 ± 0.76 µg being on the microneedle base). The loading and entrapment efficiency for coated ZMN was 2.41 ± 0.09 and 0.190 ± 0.007%, respectively. Figure 6 shows the release profiles of gemcitabine from entrapped and coated microneedles. Complete (100%) gemcitabine release was achieved from coated microneedles within 1 h. On the other hand, only 5.18 ± 0.87% (75.5 ± 12.7 µg) gemcitabine was released after 48 h from entrapped microneedles. The gemcitabine partition studies showed that 100% of the drug was retained within the aqueous release medium and did not partition into ZMN.

Skin Permeation Studies

Skin permeation studies were performed to investigate the drug disposition within the skin and permeation across the skin after application of ZMN. After 5 min insertion of ZMN in skin, the TEER was found to decrease from 3.17 ± 0.52 to 2.09 ± 0.55 kΩ. The TEWL values increased from 25.9 ± 9.7 to 32.4 ± 7.5 g/m^2/h.

Tamoxifen did not permeate across the skin after 48 h application of ZMN entrapped or coated with drug. Similarly, with the poke-and-patch approach, where the skin was pretreated with blank ZMN followed by charging tamoxifen solution, no permeation across the skin was observed. The tape stripping method was performed to remove the stratum corneum to determine the amount of tamoxifen retained

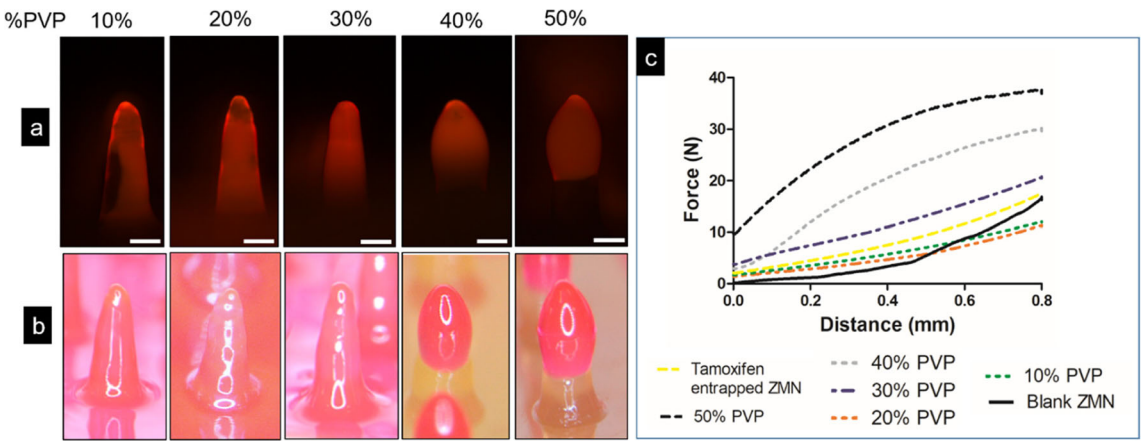

Fig. 2. **a** Fluorescence and **b** brightfield images of zein microneedles coated with different concentrations of rhodamine–PVP (scale bar = 200 µm). Compression force *versus* displacement plots for tamoxifen-loaded and blank zein microneedles

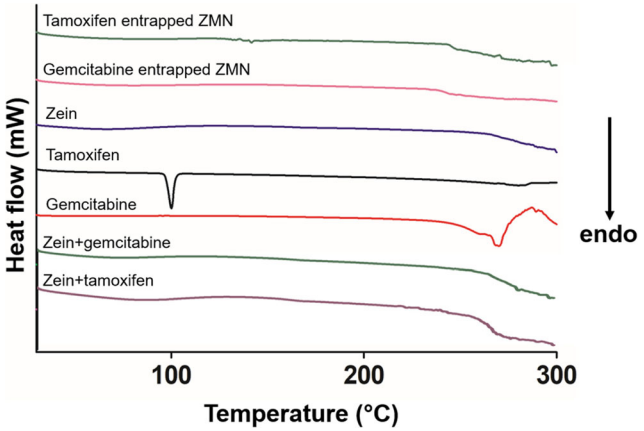

Fig. 3. DSC thermograms for neat zein, gemcitabine, tamoxifen, drug-entrapped ZMN, and physical mixtures (zein + tamoxifen and zein + gemcitabine). The physical mixtures were used with drug ratios same as that in drug-entrapped ZMN

within different skin layers. Figure 7 shows the amount of tamoxifen retained within the stratum corneum and viable epidermis. Application of tamoxifen-coated ZMN showed

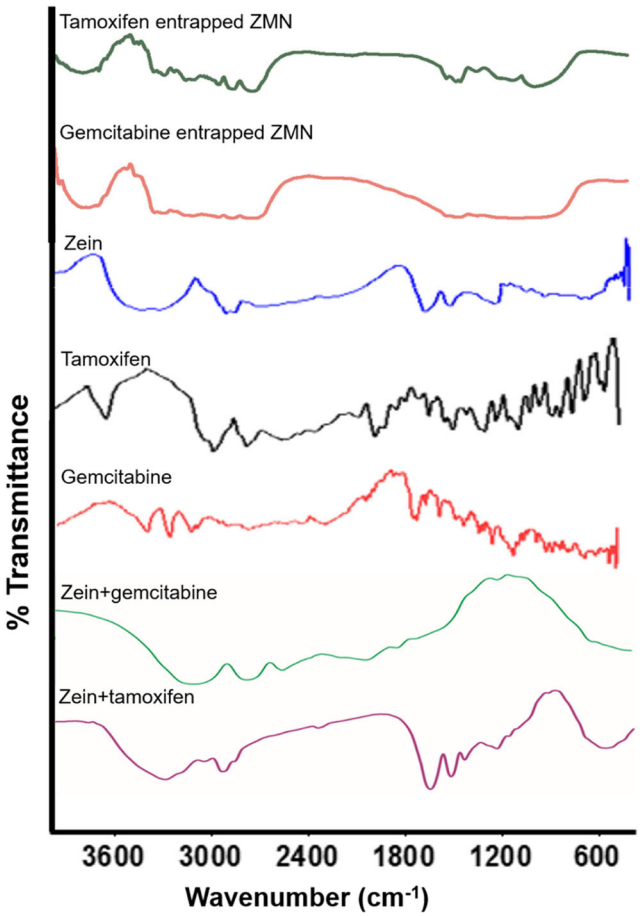

Fig. 4. Representative FTIR spectra of neat zein, gemcitabine, tamoxifen, drug-entrapped ZMN, and physical mixtures (zein + tamoxifen and zein + gemcitabine). The physical mixtures were used with drug ratios same as that in drug-entrapped ZMN

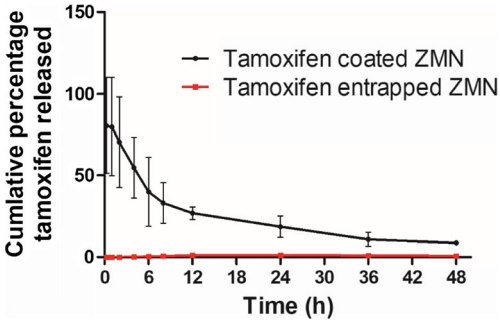

Fig. 5. Drug release profile for tamoxifen-entrapped and tamoxifen-coated zein microneedles. Release studies were performed using a Franz diffusion cell with phosphate buffer and 20% methanol as receptor media. Data presented as mean ± SD, $n = 3$

that 33.64 ± 3.58% tamoxifen (compared with loaded concentration) was retained within viable epidermis, while no drug was detected in the stratum corneum. On the other hand, only 0.23 ± 0.14% tamoxifen (compared with loaded concentration) was found in viable epidermis after insertion of tamoxifen-entrapped microneedles. With the poke-and-patch approach, 16.95 ± 3.30 and 0.52 ± 0.85% tamoxifen was recovered from viable epidermis and stratum corneum, respectively.

In the case of gemcitabine microneedles, the poke-and-patch approach provided the greatest percentage permeation across excised skin (Fig. 8a). The cumulative amount of gemcitabine permeated across the skin after 48 h was 41.48 ± 2.82 and 34.55 ± 3.09% of the loading concentration for the poke-and-patch approach and application of coated microneedles, respectively (Fig. 8a). Gemcitabine-entrapped microneedles showed 3.40 ± 0.46% of loaded concentration permeated across the skin. However, the actual amount of gemcitabine permeated after application of gemcitabine-entrapped microneedles was greater (52.18 ± 6.35 μg) compared with other strategies. This is expected as gemcitabine was also entrapped in the MN base and was available for release. Table I shows the skin permeation parameters of gemcitabine. The cumulative amount of gemcitabine permeated after 24 h application for entrapped microneedles was 81.9 ± 9.9 μg/cm^2. However, the lag time was found to be 4.9 ± 2.6 h. There was no significant difference in flux among the three application strategies.

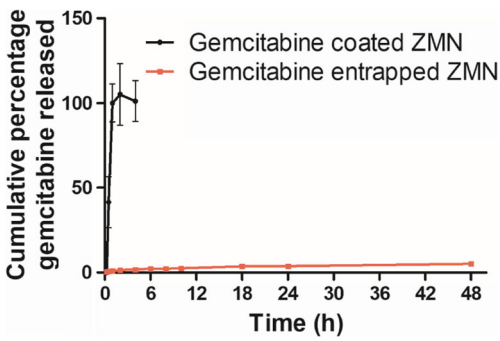

Fig. 6. Drug release profile for gemcitabine-entrapped and gemcitabine-coated zein microneedles. Release studies were performed using a Franz diffusion cell with phosphate buffer as receptor media. Data presented as mean ± SD, $n = 3$

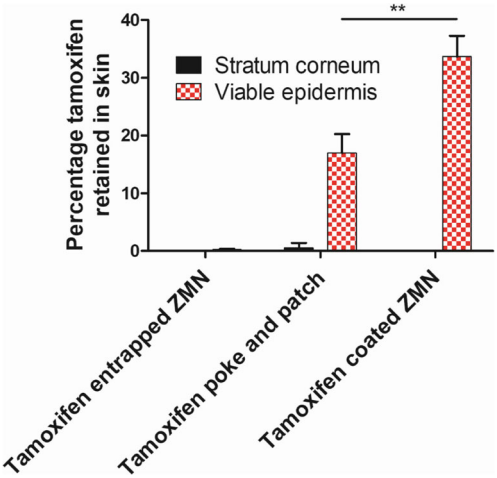

Fig. 7. Tamoxifen retained within the stratum corneum and viable epidermis after 48 h of treatment. Tamoxifen did not permeate across the skin after application of any of the formulations over 48 h. Data presented as mean ± SD, $n \geq 3$. Two asterisks are indicative of significant difference ($p < 0.05$) in the tamoxifen amount retained in viable epidermis for the poke-and-patch approach against the coated ZMN approach

Figure 8b shows the amount of gemcitabine retained within viable epidermis was 50 and 9.5% of the loaded amount after application of coated microneedles and the poke-and-patch approach. Gemcitabine was not detected within the stratum corneum after application of gemcitabine-coated ZMN.

DISCUSSION

Zein is a prolamine protein obtained from *Zea mays* (31). Zein protein has three major components, alpha, beta, and gamma (32). The alpha subunit is the major component followed by the beta and gamma subunits (33). Zein is not soluble in water because of the presence of hydrophobic residues leucine, proline, alanine, phenylalanine (total ~ 35%), and glutamic acid (~ 24%) (34–36). Zein is soluble in hydro-alcoholic mixtures containing 80–90% ethanol (37). The microneedles casted using 60% *w*/*v* zein showed sufficient mechanical strength for insertion into porcine skin (11). The compression force and skin insertion force of ZMN were reported earlier (11). While the ZMN are plastic, they are not dissolvable in aqueous medium or skin tissue (11). However, it was observed that the zein microneedles would imbibe water and swell upon prolonged incubation in aqueous medium.

Therapeutic agents can be entrapped within the matrix or coated on the microneedle surface for transdermal administration (4). Tamoxifen is an estrogen receptor modulator that competitively competes with endogenous estradiol, thereby reducing cell growth and multiplication (38). Tamoxifen shows poor water solubility of 0.04 μg/ml (21). It has fewer hydrogen bond donors and acceptors (0 and 2, respectively) (37). This hydrophobic tamoxifen appeared to be a suitable molecule to load in ZMN, where 4 mg of tamoxifen could be solubilized in 1 ml of 90% ethanol to cast microneedles. However, tamoxifen did not diffuse out of the needles into aqueous release medium. This is attributed to the poor solubility of tamoxifen in aqueous release medium. To overcome this limitation, different proportions of methanol or ethanol were mixed with release medium. This did not enhance the tamoxifen release from ZMN. To improve the rate of release, tamoxifen was surface coated on ZMN. Then again, the rate of tamoxifen release was poor when a hydrophobic polymer, ethyl cellulose, was used in coating medium for dip coating. The addition of hydrophilic PVP in the coating solution resulted in burst release of tamoxifen (80% tamoxifen released within

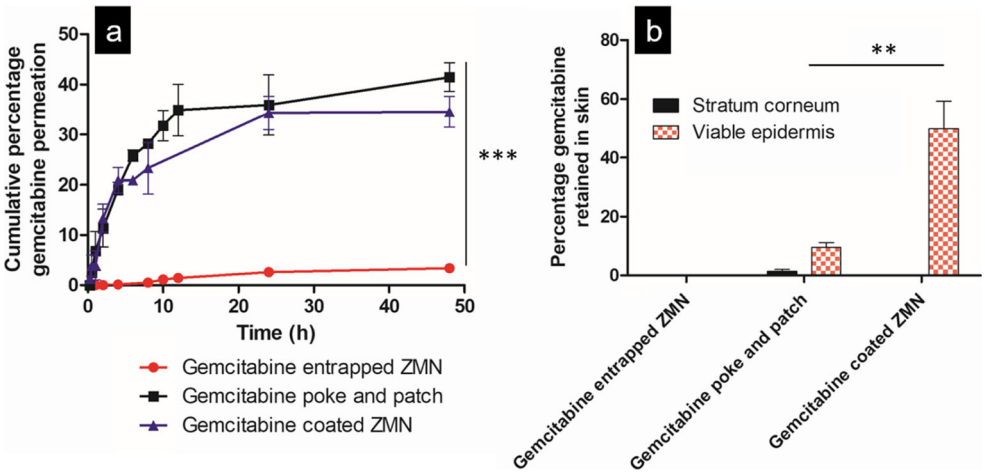

Fig. 8. **a** Gemcitabine permeation across porcine ear skin over 48 h from various ZMN formulations. Permeation studies were performed using the Franz diffusion cell. **b** Gemcitabine recovered from the stratum corneum and viable epidermis after 48 h of permeation studies. Stratum corneum was isolated using 15 tape strips (mean ± SD, $n \geq 3$). Three asterisks in **a** indicate that gemcitabine permeation across skin was significantly higher with gemcitabine-coated ZMN and the poke-and-patch approach at $p < 0.001$. Two asterisks in **b** are indicative of significant difference ($p < 0.05$) in gemcitabine amount retained in viable epidermis between coated ZMN and the poke-and-patch approach

Table I. Skin permeation parameters of gemcitabine

Treatment	Lag time (h)	J (μg/cm^2/h)	Q_{24} (μg/cm^2)	D (cm^2/h)	K_p (cm^2/h)
Gemcitabine-entrapped ZMN	4.97 ± 2.57	5.36 ± 0.83	81.92 ± 9.97	0.21 ± 0.32	0.0037 ± 0.0006
Gemcitabine-coated ZMN	0.26 ± 0.10	4.62 ± 1.35	43.39 ± 3.88	0.26 ± 0.10	0.06 ± 0.01
Gemcitabine-poke-and-patch approach	0.26 ± 0.08	8.14 ± 3.48	65.13 ± 4.42	0.48 ± 0.19	0.08 ± 0.03

ZMN zein microneedle, *J* flux, Q_{24} cumulative amount permeated at the end of 24 h per unit area, *D* diffusion coefficient, K_p permeability coefficient

15 min). The reverse partitioning of tamoxifen into ZMN can be confirmed by the partitioning studies of tamoxifen in ZMN and release medium. The tamoxifen present in the aqueous release medium of partition studies was below the detection limit of the HPLC method.

On the other hand, the highly water-soluble gemcitabine possesses seven hydrogen bond acceptors and four hydrogen bond donors (38). This greater water solubility allowed more gemcitabine release from ZMN compared with tamoxifen. Furthermore, the reverse-partitioning phenomenon observed after the release of tamoxifen was not found with gemcitabine when released from coated ZMN.

It has been documented that highly hydrophobic drugs would not significantly permeate across the skin membrane when studied using the *in vitro* diffusion cell setup (39,40). This is a drawback of the experimental setup of *in vitro* skin diffusion studies (41). The hydrophobic molecules released into the epidermal layers could be partitioned into the lipidic hypodermal layer. This would hinder its further diffusion into the aqueous release medium. Therefore, tamoxifen permeation studies showed a negligible amount of skin permeation while gemcitabine showed 34.55 ± 3.09% of the loaded dose permeated across the skin. Dermatomed skin samples with ≤ 0.5 mm thickness or epidermal membrane would be more suitable to perform skin permeation studies of hydrophobic molecules (42). In the cases where drug loading is poor in microneedles, the poke-and-patch approach could be used to improve the skin permeability. It was found that this approach is more suitable for gemcitabine than tamoxifen.

Taken together, among the three different strategies used to enhance skin permeation, the poke-and-patch approach showed greater permeation. In the case of gemcitabine, entrapped microneedle administration showed the greatest cumulative amount permeated compared with other techniques. Water solubility of chemotherapeutics would influence their loading, release behavior, and skin permeation for application using polymeric microneedles.

CONCLUSIONS

Micromolding through solvent casting can be used to prepare ZMN loaded with different small-molecule drugs. Anti-cancer agents can be either entrapped within the matrix or coated onto the surface of ZMN. While the loading of tamoxifen is more within ZMN, the release was negligible. Reverse partitioning of tamoxifen was observed after release from ZMN. A contrasting loading and release profile was shown by highly water-soluble drug, gemcitabine. Skin permeation studies showed negligible permeation of tamoxifen while gemcitabine showed greater permeation. In conclusion, optimal water solubility of drugs would provide greater skin permeation when delivered using ZMN.

ACKNOWLEDGEMENTS

This work was financially supported by BITS Pilani. The texture analyzer and multimode plate reader were procured using a grant from the Department of Science and Technology—Fund for Improvement of Science and Technology infrastructure (DST FIST).

COMPLIANCE WITH ETHICAL STANDARDS

Conflict of Interest The authors declare that they have no competing interests.

REFERENCES

1. Wang C, Ye Y, Gu Z. Local delivery of checkpoints antibodies. Hum Vaccin Immunother. 2017;13(1):245–8. https://doi.org/10.1080/21645515.2016.1223000.
2. Junwei L, Mingtao Z, Shan H, Chunyi T. Microneedle patches as drug and vaccine delivery platform. Curr Med Chem. 2017;24(22):2413–22. https://doi.org/10.2174/0929867324666170526124053.
3. Bhatnagar S, Dave K, Venuganti VVK. Microneedles in the clinic. J Control Release. 2017;260:164–82. https://doi.org/10.1016/j.jconrel.2017.05.029.
4. Kim YC, Park JH, Prausnitz MR. Microneedles for drug and vaccine delivery. Adv Drug Deliv Rev. 2012;64(14):1547–68. https://doi.org/10.1016/j.addr.2012.04.005.
5. Widera G, Johnson J, Kim L, Libiran L, Nyam K, Daddona PE, et al. Effect of delivery parameters on immunization to ovalbumin following intracutaneous administration by a coated microneedle array patch system. Vaccine. 2006;24(10):1653–64. https://doi.org/10.1016/j.vaccine.2005.09.049.
6. Bediz B, Korkmaz E, Khilwani R, Donahue C, Erdos G, Falo LD Jr, et al. Dissolvable microneedle arrays for intradermal delivery of biologics: fabrication and application. Pharm Res. 2014;31(1):117–35. https://doi.org/10.1007/s11095-013-1137-x.
7. Mikszta JA, Alarcon JB, Brittingham JM, Sutter DE, Pettis RJ, Harvey NG. Improved genetic immunization via micromechanical disruption of skin-barrier function and targeted epidermal delivery. Nat Med. 2002;8(4):415–9.
8. Indermun S, Luttge R, Choonara YE, Kumar P, du Toit LC, Modi G, et al. Current advances in the fabrication of microneedles for transdermal delivery. J Control Release. 2014;185:130–8. https://doi.org/10.1016/j.jconrel.2014.04.052.
9. Ita K. Transdermal delivery of drugs with microneedles—potential and challenges. Pharmaceutics. 2015;7(3):90–105. https://doi.org/10.3390/pharmaceutics7030090.

10. Tuan-Mahmood TM, McCrudden MT, Torrisi BM, McAlister E, Garland MJ, Singh TR, et al. Microneedles for intradermal and transdermal drug delivery. Eur J Pharm Sci. 2013;50(5):623–37. https://doi.org/10.1016/j.ejps.2013.05.005.
11. Bhatnagar S, Chawla SR, Kulkarni OP, Venuganti VVK. Zein microneedles for transcutaneous vaccine delivery: fabrication, characterization, and in vivo evaluation using ovalbumin as the model antigen. ACS Omega. 2017;2(4):1321–32. https://doi.org/10.1021/acsomega.7b00343.
12. Donnelly RF, Majithiya R, Singh TR, Morrow DI, Garland MJ, Demir YK, et al. Design, optimization and characterisation of polymeric microneedle arrays prepared by a novel laser-based micromoulding technique. Pharm Res. 2011;28(1):41–57. https://doi.org/10.1007/s11095-010-0169-8.
13. Lee JW, Han M-R, Park J-H. Polymer microneedles for transdermal drug delivery. J Drug Target. 2013;21(3):211–23. https://doi.org/10.3109/1061186X.2012.741136.
14. Park JH, Allen MG, Prausnitz MR. Polymer microneedles for controlled-release drug delivery. Pharm Res. 2006;23(5):1008–19. https://doi.org/10.1007/s11095-006-0028-9.
15. Zhu Z, Luo H, Lu W, Luan H, Wu Y, Luo J, et al. Rapidly dissolvable microneedle patches for transdermal delivery of exenatide. Pharm Res. 2014;31(12):3348–60. https://doi.org/10.1007/s11095-014-1424-1.
16. Milewski M, Brogden NK, Stinchcomb AL. Current aspects of formulation efforts and pore lifetime related to microneedle treatment of skin. Expert Opin Drug Deliv. 2010;7(5):617–29. https://doi.org/10.1517/17425241003663228.
17. Larrañeta E, Lutton REM, Woolfson AD, Donnelly RF. Microneedle arrays as transdermal and intradermal drug delivery systems: materials science, manufacture and commercial development. Mater Sci Eng R Rep. 2016;104(Supplement C):1–32. https://doi.org/10.1016/j.mser.2016.03.001.
18. Gill HS, Prausnitz MR. Coating formulations for microneedles. Pharm Res. 2007;24(7):1369–80. https://doi.org/10.1007/s11095-007-9286-4.
19. Donnelly RF, Raj Singh TR, Woolfson AD. Microneedle-based drug delivery systems: microfabrication, drug delivery, and safety. Drug Deliv. 2010;17(4):187–207. https://doi.org/10.3109/10717541003667798.
20. Shukla R, Cheryan M. Zein: the industrial protein from corn. Ind Crop Prod. 2001;13(3):171–92. https://doi.org/10.1016/S0926-6690(00)00064-9.
21. Gao S, Singh J. In vitro percutaneous absorption enhancement of a lipophilic drug tamoxifen by terpenes. J Control Release. 1998;51(2):193–9. https://doi.org/10.1016/S0168-3659(97)00168-5.
22. Fontana G, Maniscalco L, Schillaci D, Cavallaro G, Giammona G. Solid lipid nanoparticles containing tamoxifen characterization and in vitro antitumoral activity. Drug delivery. 2005;12(6):385–92. https://doi.org/10.1080/10717540590968855.
23. Heel RC, Brogden RN, Speight TM, Avery GS. Tamoxifen: a review of its pharmacological properties and therapeutic use in the treatment of breast cancer. Drugs. 1978;16(1):1–24. https://doi.org/10.2165/00003495-197816010-00001.
24. Chawla JS, Amiji MM. Biodegradable poly(ε-caprolactone) nanoparticles for tumor-targeted delivery of tamoxifen. Int J Pharm. 2002;249(1):127–38. https://doi.org/10.1016/S0378-5173(02)00483-0.
25. Jena SK, Singh C, Dora CP, Suresh S. Development of tamoxifen-phospholipid complex: novel approach for improving solubility and bioavailability. Int J Pharm. 2014;473:1):1–9. https://doi.org/10.1016/j.ijpharm.2014.06.056.
26. Aapro MS, Martin C, Hatty S. Gemcitabine—a safety review. Anti-Cancer Drugs. 1998;9(3):191–202.
27. Trickler WJ, Khurana J, Nagvekar AA, Dash AK. Chitosan and glyceryl monooleate nanostructures containing gemcitabine: potential delivery system for pancreatic cancer treatment. AAPS PharmSciTech. 2010;11(1):392–401. https://doi.org/10.1208/s12249-010-9393-0.
28. Poulin P, Chen Y-H, Ding X, Gould SE, Hop CE, Messick K, et al. Prediction of drug distribution in subcutaneous xenografts of human tumor cell lines and healthy tissues in mouse: application of the tissue composition-based model to antineoplastic drugs. J Pharm Sci. 104(4):1508–21. https://doi.org/10.1002/jps.24336.
29. Joshi G, Kumar A, Sawant K. Enhanced bioavailability and intestinal uptake of gemcitabine HCl loaded PLGA nanoparticles after oral delivery. Eur J Pharm Sci. 2014;60(Supplement C):80–9. https://doi.org/10.1016/j.ejps.2014.04.014.
30. Chitkara D, Kumar N. BSA-PLGA-based core-shell nanoparticles as carrier system for water-soluble drugs. Pharm Res. 2013;30(9):2396–409. https://doi.org/10.1007/s11095-013-1084-6.
31. Osborne TB. Classification of vegetable proteins. In: Osborne TB, editor. The vegetable proteins. New York: Longmans, Green and Co.; 1924. p. 25–35.
32. Coleman CE, Larkins BA. The prolamins of maize. In: Shewry PR, Casey R, editors. Seed proteins. The Netherlands: Kluwer Academic Publishers; 1999. p. 109–39.
33. Thompson GA, Larkins BA. Structural elements regulating zein gene expression. BioEssays. 1989;10(4):108–13. https://doi.org/10.1002/bies.950100404.
34. Wilson CM. Proteins of the kernel. In: Watson SA, Ramstad PE, editors. Corn: chemistry and technology. St. Paul: Am. Assoc. Cereal Chem; 1987. p. 273–310.
35. Paliwal R, Palakurthi S. Zein in controlled drug delivery and tissue engineering. J Control Release. 2014;189:108–22.
36. Jane J, Lim S, Paetau I, Spence K, Wang S. Biodegradable plastics made from agricultural biopolymers. ACS Publications; 1994.
37. Lawton JW. Zein: a history of processing and use. Cereal Chem J. 2002;79(1):1–18. https://doi.org/10.1094/CCHEM.2002.79.1.1.
38. Clemons M, Danson S, Howell A. Tamoxifen ('Nolvadex'): a review: antitumour treatment. Cancer Treat Rev. 2002;28(4):165–80.
39. Bhatia A, Kumar R, Katare OP. Tamoxifen in topical liposomes: development, characterization and in-vitro evaluation. J Pharm Pharm Sci. 2004;7(2):252–9.
40. Manosroi A, Kongkaneramit L, Manosroi J. Stability and transdermal absorption of topical amphotericin B liposome formulations. Int J Pharm. 2004;270(1):279–86. https://doi.org/10.1016/j.ijpharm.2003.10.031.
41. Ng S-F, Rouse JJ, Sanderson FD, Meidan V, Eccleston GM. Validation of a static Franz diffusion cell system for in vitro permeation studies. AAPS PharmSciTech. 2010;11(3):1432–41. https://doi.org/10.1208/s12249-010-9522-9.
42. Williams FM. In vitro studies—how good are they at replacing in vivo studies for measurement of skin absorption? Environ Toxicol Pharmacol. 2006;21(2):199–203. https://doi.org/10.1016/j.etap.2005.07.009.